IOP Publishing Journal of Physics: Condensed Matter
J. Phys.: Condens. Matter **32** (2020) 204002 (9pp) https://doi.org/10.1088/1361-648X/ab6cc2

Spin-crossover in iron(II)-phenylene ethynylene-2,6-di(pyrazol-1-yl) pyridine hybrids: toward switchable molecular wire-like architectures

Kuppusamy Senthil Kumar[1], Ivan Šalitroš[2,3,4], Benoît Heinrich[1], Simona Moldovan[5], Matteo Mauro[1] and Mario Ruben[1,6]

[1] Institut de Physique et Chimie des Matériaux de Strasbourg (IPCMS), CNRS-Université de Strasbourg, 23, rue du Loess, BP 43, 67034 Strasbourg cedex 2, France
[2] Faculty of Chemical and Food Technology, Department of Inorganic Chemistry, Slovak University of Technology, Bratislava 81237, Slovakia
[3] Faculty of Science, Department of Inorganic Chemistry, Palacký University, 17. listopadu 12, 771 46 Olomouc, Czech Republic
[4] Central European Institute of Technology, Brno University of Technology, Purkyňova 123, 61200 Brno, Czech Republic
[5] Groupe de Physique des Matériaux (GPM), UMR 6634, CNRS–Université de Normandie–INSA de Rouen, Avenue de l'Université—BP12, 76801 Saint Etienne du Rouvray, France
[6] Institute of Nanotechnology, Karlsruhe Institute of Technology (KIT), Hermann-von-Helmholtz-Platz 1, 76344, Eggenstein-Leopoldshafen, Germany

E-mail: senthil.kuppusamy@ipcms.unistra.fr, matteo.mauro@ipcms.unistra.fr and mario.ruben@kit.edu

Received 29 October 2019, revised 17 December 2019
Accepted for publication 16 January 2020
Published 18 February 2020

Abstract

Luminescent oligo(p-phenylene ethynylene) (OPE) and spin-crossover (SCO) active Fe(II)-2,6-di(pyrazol-1-yl) pyridine (BPP) systems are prominent examples proposed to develop functional materials such as molecular wires/memories. A marriage between OPE and Fe(II)-BPP systems is a strategy to obtain supramolecular luminescent ligands capable of metal coordination useful to produce novel spin-switchable hybrids with synergistic coupling between spin-state of Fe(II) and a physical property associated with the OPE skeleton, for example, electronic conductivity or luminescence. To begin in this direction, two novel ditopic ligands, namely L^1 and L^2, featuring OPE-type backbone end-capped with metal coordinating BPP were designed and synthetized. The ligand L^2 tailored with 2-ethylhexyloxy chains at the 2 and 5 positions of the OPE skeleton shows modulated optical properties and improved solubility in common organic solvents relative to the parent ligand L^1. Solution phase complexation of L^1 and L^2 with $Fe(BF_4)_2{\cdot}6H_2O$ resulted in the formation of insoluble materials of the composition $[Fe(L^1)]_n(BF_4)_{2n}$ and $[Fe(L^2)]_n(BF_4)_{2n}$ as inferred from elemental analyses. Complex $[Fe(L^1)]_n(BF_4)_{2n}$ underwent thermal SCO centred at $T_{1/2} = 275$ K as well as photoinduced low-spin to high-spin transition with the existence of the metastable high-spin state up to 52 K. On the other hand, complex $[Fe(L^2)]_n(BF_4)_{2n}$, tethered with 2-ethylhexyloxy groups, showed gradual and half-complete SCO with 50% of the Fe(II)-centres permanently

blocked in the high-spin state due to intermolecular steric interactions. The small angle x-ray scattering (SAXS) pattern of the as-prepared solid complex $[Fe(L^1)]_n(BF_4)_{2n}$ revealed the presence of nm-sized crystallites implying a possible methodology towards the template-free synthesis of functional-SCO nanostructures.

Keywords: molecular magnetism, spin-crossover, functional materials

S Supplementary material for this article is available online

(Some figures may appear in colour only in the online journal)

1. Introduction

Functional molecular/polymeric materials are at the forefront of materials chemistry research due to their diverse applicability, especially in nanotechnology [1–15]. Spin-crossover (SCO) complexes showing cooperative/bi-stable SCO behaviour are proposed candidates to obtain molecule-based switching and memory elements due to their reversible interconversion between low-spin (LS) and high-spin (HS) states effected by external stimuli [16–24]. Fe(II) complexes based on 2,6-di(pyrazol-1-yl)pyridine (BPP) ligands are a well-studied class of SCO complexes due to their facile propensity to undergo SCO around room temperature (RT) [25–29]. On the other hand, oligo(p-phenylene ethynylene) (OPE) derivatives feature alluring electronic and optical properties. A range of OPE-based ligands composed of bipyridine (bpy) or terpyridine (tpy) metal-binding motifs have been reported, and the utility of the resultant metal-OPE complexes as molecular wires and light-responsive supramolecular gel-forming materials have been demonstrated [30–44]. In this context, designing OPE-BPP hybrid ligands and their complexation with Fe(II) is a strategy to obtain novel SCO-molecular wire-like hybrids with possible synergetic coupling between spin-state and electrical conductance [45–53]. To start exploring towards realizing switchable molecular-wire like hybrids, two novel OPE-BPP- based ditopic ligands—L^1 and L^2—were designed and synthesized as depicted in chart 1.

The ligand L^2 was designed, by appending branched 2-ethylhexyloxy side chains at the 2 and 5 positions of the parent ditopic OPE-BPP ligand skeleton. The introduction of the 2-ethylhexyloxy side chains is expected to improve the solubility, modulate the optoelectronic characteristics, and tune the spin-state switching behaviour of the corresponding Fe(II) complex—$[Fe(L^2)]_n(BF_4)_{2n}$. The ditopic nature of the OPE-BPP ligands discussed in this study is appealing to construct M^{2+}-BPP (M = Fe, Ru, etc) systems [54, 55] with materials application potential—a rather unexplored area, as recently reviewed by Attwood and Turner [56]. In the following sections, the structure-property relationships associated with ligands L^1 and L^2 and the corresponding Fe(II) complexes—$[Fe(L^m)]_n(BF_4)_{2n}$, $m = 1$ or 2—are discussed. The lateral organization of the complex entities in their powder forms was investigated by performing small angle x-ray scattering (SAXS) measurements. A combination of SAXS and tunnelling electron microscopy (TEM) experiments were used to probe the nanostructured nature of the deposits of $[Fe(L^1)]_n(BF_4)_{2n}$.

2. Results and discussion

2.1. Synthesis of the ligands and complexes

Ligands L^1 and L^2 were synthesised by performing classical Sonogashira coupling reaction [57] between the precursor diethynyl-benzene derivatives (1.1 or 1.2, scheme 1) [58] and 4-Iodo-2,6-di-pyrazol-1-yl-pyridine (1.3, scheme 1) [54].

The target 1D-complexes were prepared by treating one equivalent of $Fe(BF_4)_2{\cdot}6H_2O$ with one equivalent of L^1/L^2 dissolved in the dichloromethane solvent. Based on our previous observation [55] and elemental analyses, we assume the structure of the resulting Fe(II) complexes as oligomeric/polymeric 1D-architectures with the probable molecular formula $[Fe(L^m)]_n(BF_4)_{2n}$, $m = 1$ or 2.

The complexes are insoluble in common organic solvents, caused by contrasting solubility behaviour arising from the combination polar Fe(II) core and non-polar/hydrophobic branched alkyl chains and OPE backbone. The possible presence of solvent end-capped Fe(II) coordination sites could be another factor rendering the complexes insoluble.

2.2. Photophysical properties of the ligands and complexes

Electronic absorption spectroscopic (UV–vis) studies of the ligands L^1 and L^2 in dichloromethane solvent revealed predominantly OPE-based electronic transitions in the 250–400 nm spectral region in line with the literature reports detailing absorption characteristics of OPE-type ditopic-chelating ligands [37, 59, 60]. Ligand L^2 showed features attributable to the electronic properties induced by the bis-alkoxy substitution of the central aromatic ring [61]. As far

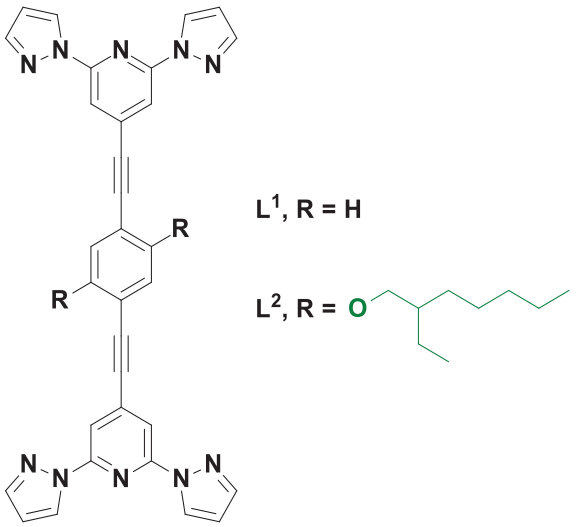

Chart 1. The ditopic OPE-BPP ligands—L^1 and L^2—used to prepare SCO complexes reported in this study.

as ligand L^1 is concerned, its absorption spectrum displays an intense ($\varepsilon = \sim 1.2 \times 10^5$ M^{-1} cm^{-1}) band at 327 nm that is ascribed to the $^1\pi - \pi^*$ transition extending over the ligand scaffold. Two main bands characterize the corresponding absorption spectrum for ligand L^2 instead. At higher energy, a $^1\pi - \pi^*$ transition similar to L^1 is present at $\lambda_{abs,max} = 326$ nm, although with much lower intensity ($\varepsilon = \sim 3.2 \times 10^4$ M^{-1} cm^{-1}) when compared with L^1. At lower energy, a featureless band is present with similar intensity ($\lambda_{abs,max} = 389$ nm, $\varepsilon = \sim 1.9 \times 10^4\,M^{-1}\,cm^{-1}$) suggesting an intramolecular electronic transition with partial charge transfer (CT) character. As a result, an overall reduced optical band gap is observed for L^2 compared with L^1. Going from solution to solid-state, bathochromic shift of the absorption maxima is observed for the ligands attributable to the establishment of intermolecular $\pi - \pi$ interactions in the condensed phase (figure S1).

Photo-irradiation of CH_2Cl_2 solutions of the ligands at their respective lower energy absorption maxima resulted in bright luminescence (figure 1(a)) with $\lambda_{em,max} = 376$ nm (L^1) and 443 nm (L^2). Ligand L^1 displays emission features that mirror the lowest-energy absorption band; the emission could be ascribed to a radiative transition from a $^1\pi - \pi^*$ localized excited state (LE). Instead, L^2 shows a structured and broader profile most likely due to partial CT state admixed with the LE state. Moreover, 2-ethylhexyloxy substitution at the OPE skeleton enhanced photoluminescence quantum yield (PLQY) of L^2 compared with L^1, see table 1. Excitation spectra trace out the corresponding absorption profile (figure S2). The insoluble nature of the Fe(II) complexes prohibited photophysical studies in solution.

Solid-state photoluminescence studies of the ligands, upon excitation at their respective lower energy solid-state absorption maxima (figure S1), revealed broader emission bands (figure 1(b)) in comparison with the solution state features of the ligands. The Fe(II) complexes are also emissive in the solid-state; a probable origin of emission is the uncoordinated ligand end groups.

2.3. Spin-crossover behaviour of the complexes

At 400 K, a χT value of ~3.25 cm^3 mol^{-1} K (figure 2(a), black circles) was obtained for $[Fe(L^1)]_n(BF_4)_{2n}$, indicating the existence of pure HS-state of the Fe(II) centre at that temperature. Upon cooling, a gradual decrease of the χT product function was observed. At 5 K, a χT value of ~0.5 cm^3 mol^{-1} K was obtained, thus indicating a predominantly LS-state of the complex (see figure S3 also). The residual magnetic moment could be attributed either to the HS-state of the end-capped Fe(II) coordination sites in line with our previous report detailing similar 1D-SCO system [55] and/or to the residual HS-fraction (≈18%). Overall, a gradual thermal SCO with $T_{1/2} = 275$ K is observed for $[Fe(L^1)]_n(BF_4)_{2n}$.

The complex is also light induced excited spin-state trapping (LIESST) active, and a red-light irradiation ($\lambda = 637$ nm) at 10 K transformed it into the metastable HS state (figure 2(a), blue triangles). The photoexcitation is almost quantitative, and a T(LIESST) = 52 K (figure 2(a), inset) is observed. The relaxation of metastable HS fraction of the complex upon the increase of temperature (LIESST curve; purple squares) showed a rather non-cooperative character in line with the gradual shape of the thermally induced SCO curve [62].

The complex $[Fe(L^2)]_n(BF_4)_{2n}$, featuring branched 2-ethylhexyloxy chains at the backbone showed a χT value of ~2.9 cm^3 K mol^{-1} at 400 K, attributed to almost HS state of Fe(II)-centres (figure 2(b), red circles). Upon cooling, the χT product function decreased gradually and at 50 K, $\chi T = 1.7$ cm^3 K mol^{-1} is observed, indicating the coexistence of almost equal proportions of LS- and residual HS Fe(II) fractions.

2.4. Small-angle x-ray scattering (SAXS) and transmission electron microscopy (TEM) studies of the complexes

To shed light on the lateral organisation of the complex entities in the lattice, SAXS experiments were carried out, as depicted in figure 3.

The parent complex $[Fe(L^1)]_n(BF_4)_{2n}$ showed broadened reflections, evidencing a crystalline state with small crystallites of about 10 nm size. Introduction of ramified alkyl sidechains strongly hampered crystallisation and the complex $[Fe(L^2)]_n(BF_4)_{2n}$ was found to be merely amorphous. The SAXS pattern is indeed dominated by the intense wide-angle scattering from lateral distances between molten alkyl chains (h_{ch}) and liquid-like lateral distances between backbones in amorphous domains (h_c), besides a few weak and broadened reflections from rare and small-size crystallized domains (figure 3, blue trace).

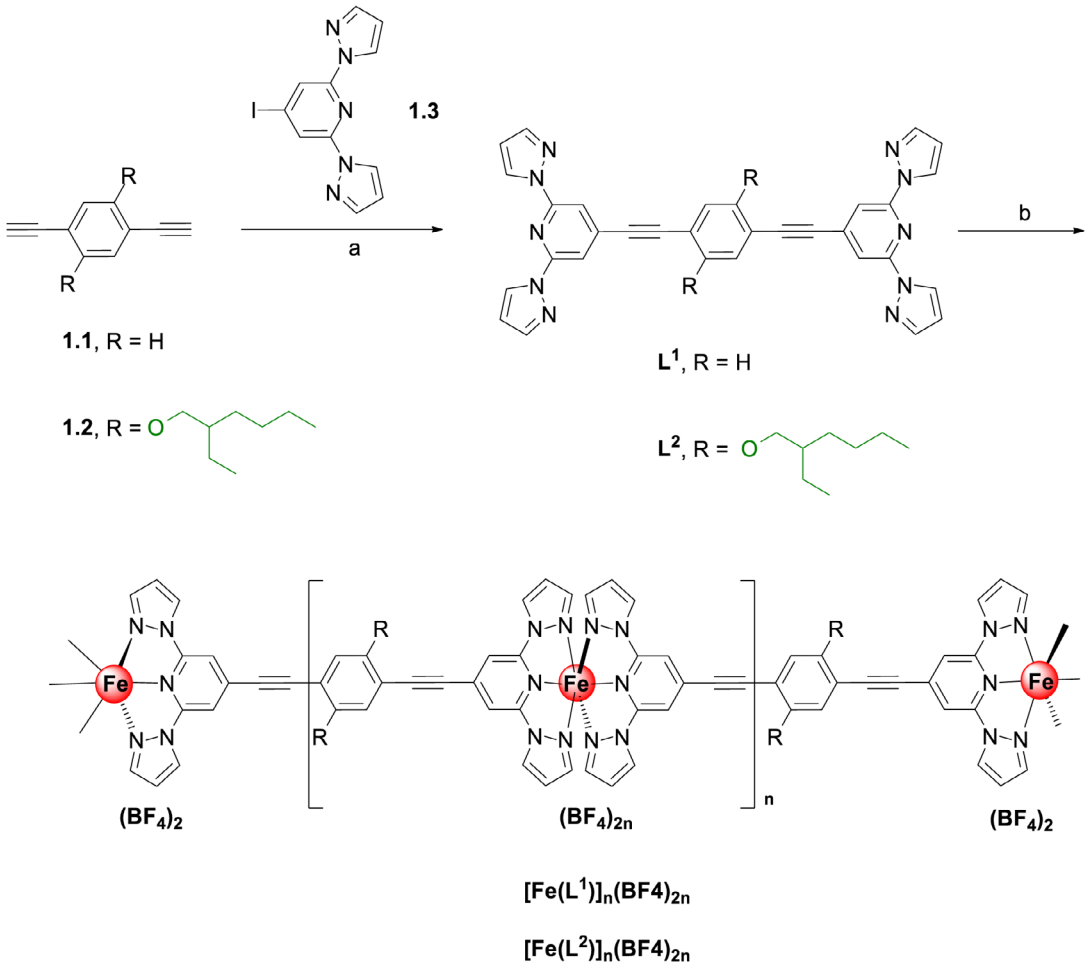

Scheme 1. Synthesis of OPE-BPP ligands L^1 and L^2 and the corresponding 1D-Fe(II) complexes. Reagents and conditions: (a) $PdCl_2(PPh_3)_2$, CuI, THF/Et_3N, Ar, 60 °C, 12 h and (b) $Fe(BF_4)_2{\cdot}6H_2O$, DCM/ACN, Ar, RT, 72 h. See supporting information for detailed experimental procedures.

The nanostructure formation inferred from SAXS for $[Fe(L^1)]_n(BF_4)_{2n}$ was probed by TEM. The TEM studies showed a random organisation of the complex crystallites with superimposed nanograins of sizes superior to 50 nm, as depicted in figure 4. The *Z*-contrast developed under the high angular annular dark-field detection (HAADF) allowed to unambiguously identify the presence of nano-sized and irregularly shaped architectures, which are uniformly distributed on the surface (figure 4(b)). The mean grain size is 10 nm, in consistency with the crystallite size from SAXS.

Table 1. Photophysical data recorded for the ligand L^1 and L^2 in CH_2Cl_2 solvent at room temperature.

Entry	$\lambda_{max,abs}$ (ε) (nm, (10^4 M^{-1} cm^{-1}))	λ_{em} (nm)	PLQY[a] (%)
L^1	270 (4.63), 327 (11.96), 348[*sh*] (8.91), 380 (0.20)	376	27
L^2	270 (2.28), 3.16 (3.00), 326 (3.17), 389 (1.92)	443	78

sh denotes shoulder.
[a] Determined by relative method using 0.5 M quinine sulphate in aqueous H_2SO_4 as the reference standard.

3. Discussion

The present study is important in terms of realizing functional SCO complexes. The model complex $[Fe(L^1)]_n(BF_4)_{2n}$ gave indeed raise to a gradual but almost complete SCO. One notes that the spin-state switching occurs without any apparent hysteresis and with reduced $T_{1/2}$ values compared to previous 1D-coordination polymer reported from our group [55]. On the contrary, the 2-ethylhexyloxy substituted $[Fe(L^2)]_n(BF_4)_{2n}$ complex showed a hampered spin-state transformation during the heating and cooling cycles leading to incomplete SCO. As verified by SAXS, the ramified alkyl chains are molten and come down to a liquid that spaces the backbones and confers them the freedom to move one with respect to each other, explaining the overall amorphous state of $[Fe(L^2)]_n(BF_4)_{2n}$ complex. Hence, the transition to the ordered LS state is delayed and ultimately never reached; this is likely the main reason behind the incomplete SCO behavior of this complex.

Despite the above-discussed shortcomings, the results obtained in this study are encouraging to design novel 1D-SCO coordination networks based on the OPE-BPP skeleton. The

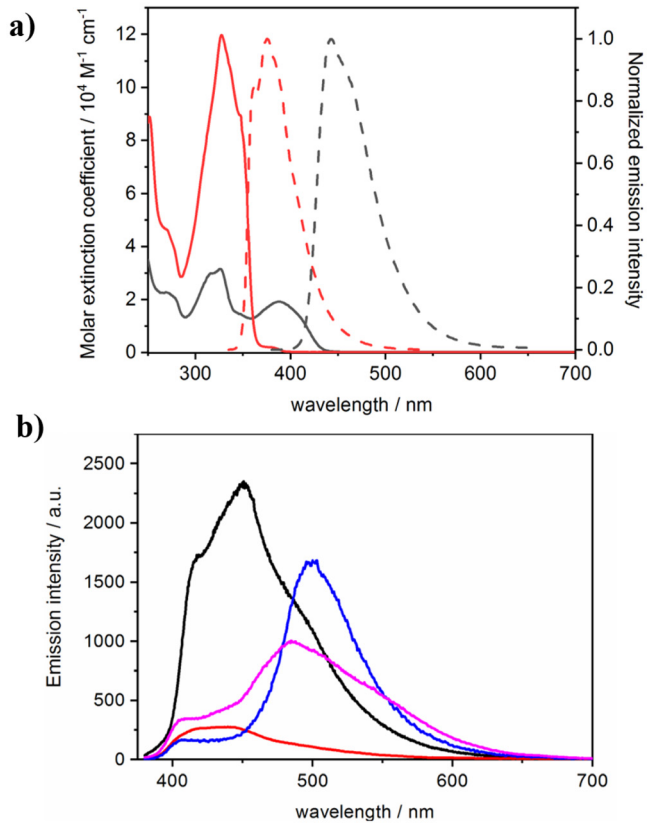

Figure 1. (a) Electronic absorption (solid traces) and photoluminescence (dashed traces) spectra of L^1 (red) and L^2 (black) in air-equilibrated CH_2Cl_2 solution at a concentration of 1.0×10^{-5} M at room temperature. Emission spectra were recorded upon excitation at $\lambda_{exc} = 300$ and 360 nm for L^1 and L^2, respectively and (b) solid-state photoluminescence (PL) spectra of L^1 (black), L^2 (blue), $[Fe(L^1)]_n(BF_4)_{2n}$ (red) and $[Fe(L^2)]_n(BF_4)_{2n}$ (magenta); see figure S1 for the corresponding absorption spectra in the solid state.

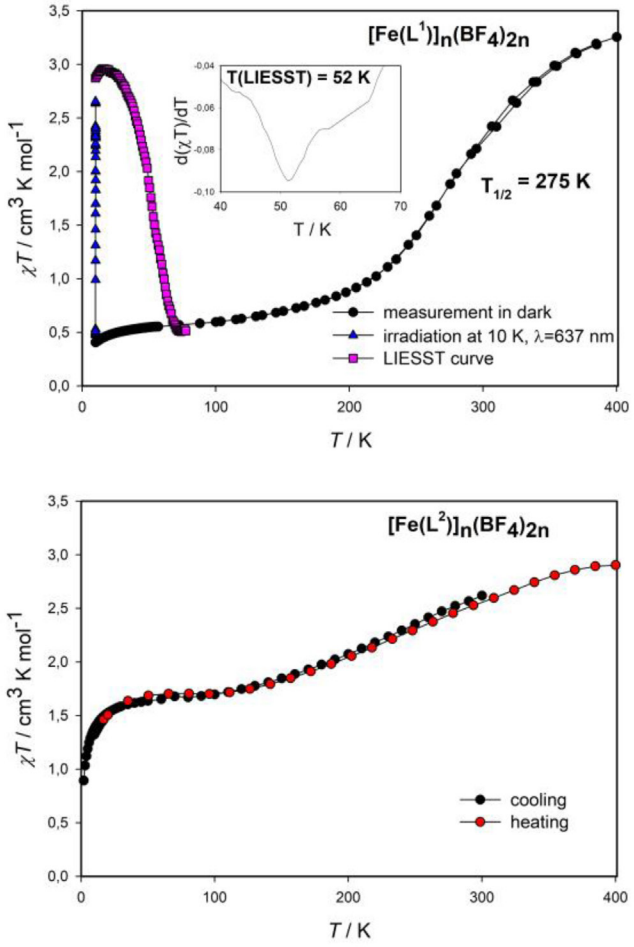

Figure 2. Spin-crossover behaviour of the complexes. (a) $[Fe(L^1)]_n(BF_4)_{2n}$; the black circles represent T versus χT product, blue triangles represent increase of χT product under 637 nm light irradiation at 10 K, and purple squares represents evolution of χT in the absence of light irradiation. The inset shows $d(\chi T)/dT$ plot indicating T(LIESST) = 52 K. (b) χT versus T plot of $[Fe(L^2)]_n(BF_4)_{2n}$, the black and red circles represent cooling and heating branches of χT versus T plot, respectively.

emphasis should be on the judicious choice of spacer/solubilizing groups, which should confer solution processability without blocking SCO. This is in particular necessary for the envisioned SCO active molecular wire-like architectures with tuneable conductance [32, 63–66]. Otherwise, the model SCO complexes detailed in this study could be modified, via synthetic ligand engineering, with suitable functional groups to develop molecular materials with novel functions. For example, by appending donor and acceptor groups at the sides of the molecular wire-like oligomeric network bridged by the SCO active sites, spin-state dependence of electron transport could be studied by manipulating the supramolecular system by light or temperature stimulus [67, 68]. In another scenario, self-assembled monolayers (SAM) composed of electron acceptor units, electron donor units, and SCO centres could be fabricated on top of a metallic electrode by employing layer by layer (LBL) self-assembly methods, and their electron transfer properties with respect to spin-state could be studied [69–74]. Systematic studies in the above discussed challenging directions may lead to interesting results of fundamental and applied scientific importance.

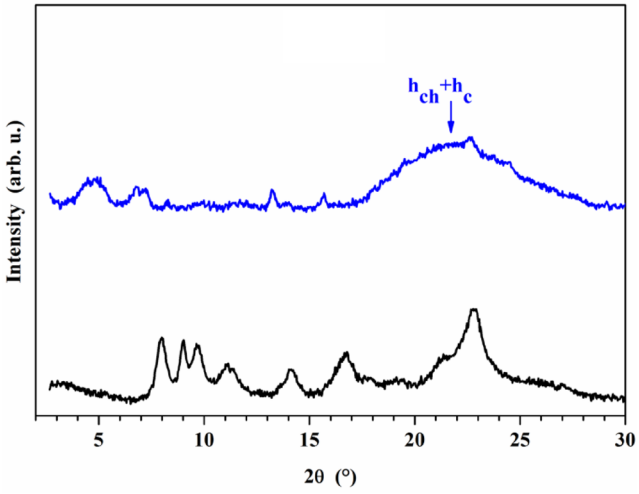

Figure 3. SAXS patterns of complexes $[Fe(L^1)]_n(BF_4)_{2n}$ (black trace) and $[Fe(L^2)]_n(BF_4)_{2n}$ (blue trace) at 293 K.

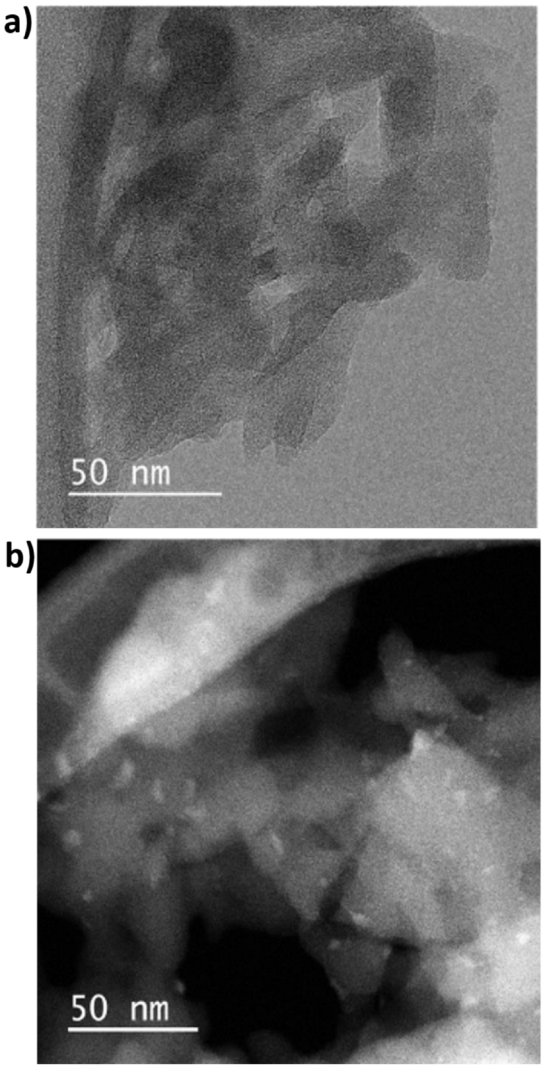

Figure 4. TEM and STEM micrographs of $[Fe(L^1)]_n(BF_4)_{2n}$ complex acquired under (a) bright field and (b) high angular annular dark field (HAADF) modes.

4. Conclusions

A set of 1D-SCO complexes featuring luminescent OPE-BPP ligand systems were designed, synthesised, and their spin-state switching behaviour were investigated. While $[Fe(L^1)]_n(BF_4)_{2n}$ showed a gradual and near-complete SCO, the branched alkyl chain tethered complex $[Fe(L^2)]_n(BF_4)_{2n}$ showed incomplete switching attributed to the steric interaction mediated blocking of the SCO. Moreover, the gradual—spanning a large temperature window—and incomplete nature of SCO in parent and functionalized complex, respectively, render them unfit to study a synergistic coupling between SCO and luminescence. The insoluble nature of the complexes proved to be a difficulty in processing them for applications; the emphasis should be more on the judicious choice of spacer/solubilising groups to confer suitable processability from solution. Despite these shortcomings, the SCO of the complexes detailed in this study could be a useful stepping-stone to develop molecular materials with novel functions. For instance, the realisation of soluble 1D-polymeric/oligomeric SCO complexes may lead to the observation of spin-state dependence of electron transport in molecular wire-like systems, which would be of importance in molecular electronics [75–84].

The functionalization of the OPE backbone with 2-ethylhexyloxy side chains resulted in about three fold increase of the PLQY for L^2 when compared with L^1 in the solution-state. A more detailed investigation of the photophysical properties of the ligands in solution, such as concentration and solvent polarity effect studies, and solid-states is necessary to understand the photophysical properties of this novel OPE-BPP ligand systems.

The observation of nano-sized architectures of $[Fe(L^1)]_n(BF_4)_{2n}$ is interesting in view of the reports detailing the delamination of bulk crystalline architectures into 2D nm thick films [85–87]. A careful elucidation of size dependence of SCO behaviour of nanosized materials obtained from delamination/exfoliation of bulk SCO active crystalline materials is the need of the hour. Such elucidations might lead to nanosized spin-switchable systems suitable for applications [88–94].

Acknowledgments

Grant Agency Innovation FRC is acknowledged for the financial support for the project Self-assembly of spin-crossover (SCO) complexes on graphene. M.R. thanks the DFG priority program 1928 ‘COORNETS’ for generous support. IŠ acknowledges the financial support from Slovak grant agencies (APVV-18-0197, APVV-18-0016, VEGA 1/0125/18), from institutional sources of the Department of Inorganic Chemistry, Palacký University Olomouc, Czech Republic and from Ministry of Education, Youth and Sports of the Czech Republic under the project CEITEC 2020 (LQ1601) are acknowledged for the financial support. GENESIS is supported by the Région Haute-Normandie, the Métropole Rouen Normandie, the CNRS via LABEX EMC and the French National Research Agency as a part of the program ‘Investissements d’avenir’ with the reference ANR-11-EQPX-0020.

ORCID iDs

Kuppusamy Senthil Kumar https://orcid.org/0000-0002-1501-7759
Benoît Heinrich https://orcid.org/0000-0001-6795-2733
Mario Ruben https://orcid.org/0000-0002-7718-7016

References

[1] Fourmigué M and Ouahab L 2009 *Conducting and Magnetic Organometallic Molecular Materials* (Berlin: Springer)
[2] Coronado E, Galán-Mascarós J R, Gómez-García C J and Laukhin V 2000 Coexistence of ferromagnetism and metallic conductivity in a molecule-based layered compound *Nature* **408** 447–9
[3] Gatteschi D 1991 *Magnetic Molecular Materials* (Dordrecht: Academic)
[4] Sagara Y, Yamane S, Mitani M, Weder C and Kato T 2016 Mechanoresponsive luminescent molecular assemblies: an emerging class of materials *Adv. Mater.* **28** 1073–95

[5] Sieklucka B and Pinkowicz D 2017 *Molecular Magnetic Materials: Concepts and Applications* (Weinheim: Wiley)
[6] Gatteschi D 1994 Molecular magnetism: a basis for new materials *Adv. Mater.* **6** 635–45
[7] Liu Z 2003 Molecular memories that survive silicon device processing and real-world operation *Science* **302** 1543–5
[8] Gaita-Ariño A, Luis F, Hill S and Coronado E 2019 Molecular spins for quantum computation *Nat. Chem.* **11** 301–9
[9] Wang Y, Sun L, Wang C, Yang F, Ren X, Zhang X, Dong H and Hu W 2019 Organic crystalline materials in flexible electronics *Chem. Soc. Rev.* **48** 1492–530
[10] Shirota Y 2005 Photo- and electroactive amorphous molecular materials—molecular design, syntheses, reactions, properties, and applications *J. Mater. Chem.* **15** 75–93
[11] Ratera I and Veciana J 2012 Playing with organic radicals as building blocks for functional molecular materials *Chem. Soc. Rev.* **41** 303–49
[12] Pianowski Z L 2019 Recent implementations of molecular photoswitches into smart materials and biological systems *Chem. Eur. J.* **25** 5128–44
[13] Merino E 2011 Synthesis of azobenzenes: the coloured pieces of molecular materials *Chem. Soc. Rev.* **40** 3835
[14] Wernsdorfer W and Ruben M 2019 Synthetic hilbert space engineering of molecular Qu *d* its: isotopologue chemistry *Adv. Mater.* **31** 1806687
[15] Rocha A R, García-suárez V M, Bailey S W, Lambert C J, Ferrer J and Sanvito S 2005 Towards molecular spintronics *Nat. Mater.* **4** 335–9
[16] Kahn O 1998 Spin-transition polymers: from molecular materials toward memory devices *Science* **279** 44–8
[17] Kahn O, Kröber J and Jay C 1992 Spin transition molecular materials for displays and data recording *Adv. Mater.* **4** 718–28
[18] Weber B, Bauer W and Obel J 2008 An iron(II) spin-crossover complex with a 70 K wide thermal hysteresis loop *Angew. Chem., Int. Ed. Engl.* **47** 10098–101
[19] Halcrow M A 2014 Spin-crossover compounds with wide thermal hysteresis *Chem. Lett.* **43** 1178–88
[20] Cobo S, Molnár G, Real J A and Bousseksou A 2006 Multilayer sequential assembly of thin films that display room-temperature spin crossover with hysteresis *Angew. Chem., Int. Ed. Engl.* **45** 5786–9
[21] Bousseksou A, Molnár G, Demont P and Menegotto J 2003 Observation of a thermal hysteresis loop in the dielectric constant of spin crossover complexes: towards molecular memory devices *J. Mater. Chem.* **13** 2069–71
[22] Senthil Kumar K and Ruben M 2017 Emerging trends in spin crossover (SCO) based functional materials and devices *Coord. Chem. Rev.* **346** 176–205
[23] Madhu N T, Salitros I, Schramm F, Klyatskaya S, Fuhr O and Ruben M 2008 Above room temperature spin transition in a series of iron(II) bis(pyrazolyl)pyridine compounds *C. R. Chim.* **11** 1166–74
[24] Thomas Madhu N, Knittl E T, Desalegn Zeleke T, Gonfa Robi A and Linert W 2017 Room-temperature spin-transition iron compounds *J. Chem. Appl. Chem. Eng.* **01**
[25] Holland J M, Kilner C A, Thornton-Pett M, Halcrow M A, McAllister J A and Lu Z 2001 An unusual abrupt thermal spin-state transition in $[FeL^2][BF_4]_2$ [L = 2,6-di(pyrazol-1-yl)pyridine] *Chem. Commun.* 577–8
[26] Halcrow M A 2009 Iron(II) complexes of 2,6-di(pyrazol-1-yl) pyridines—a versatile system for spin-crossover research *Coord. Chem. Rev.* **253** 2493–514
[27] Kershaw Cook L J, Mohammed R, Sherborne G, Roberts T D, Alvarez S and Halcrow M A 2015 Spin state behavior of iron(II)/dipyrazolylpyridine complexes. New insights from crystallographic and solution measurements *Coord. Chem. Rev.* **289–90** 2–12
[28] Halcrow M A 2011 Structure:function relationships in molecular spin-crossover complexes *Chem. Soc. Rev.* **40** 4119
[29] Halcrow M A, Capel Berdiell I, Pask C M and Kulmaczewski R 2019 Relationship between the molecular structure and switching temperature in a library of spin-crossover molecular materials *Inorg. Chem.* **58** 9811–21
[30] Linton K E, Fox M A, Pålsson L-O and Bryce M R 2015 Oligo(*p* -phenyleneethynylene) (OPE) molecular wires: synthesis and length dependence of photoinduced charge transfer in OPEs with triarylamine and diaryloxadiazole end groups *Chem. Eur. J.* **21** 3997–4007
[31] Zhao X, Huang C, Gulcur M, Batsanov A S, Baghernejad M, Hong W, Bryce M R and Wandlowski T 2013 Oligo(aryleneethynylene)s with terminal pyridyl groups: synthesis and length dependence of the tunneling-to-hopping transition of single-molecule conductances *Chem. Mater.* **25** 4340–7
[32] Wielopolski M, Atienza C, Clark T, Guldi D M and Martín N 2008 *p* -phenyleneethynylene molecular wires: influence of structure on photoinduced electron-transfer properties *Chem. Eur. J.* **14** 6379–90
[33] Hortholary C and Coudret C 2003 An approach to long and unsubstituted molecular wires: synthesis of redox-active, cationic phenylethynyl oligomers designed for self-assembled monolayers *J. Org. Chem.* **68** 2167–74
[34] Xiao X, Nagahara L A, Rawlett A M and Tao N 2005 Electrochemical gate-controlled conductance of single oligo(phenylene ethynylene)s *J. Am. Chem. Soc.* **127** 9235–40
[35] Herrer L, Ismael A, Martín S, Milan D C, Serrano J L, Nichols R J, Lambert C and Cea P 2019 Single molecule versus large area design of molecular electronic devices incorporating an efficient 2-aminepyridine double anchoring group *Nanoscale* **11** 15871–80
[36] Grosshenny V, Romero F M and Ziessel R 1997 Construction of preorganized polytopic ligands via palladium-promoted cross-coupling reactions *J. Org. Chem.* **62** 1491–500
[37] Grosshenny V, Harriman A and Ziessel R 1995 Electronic energy transfer across ethynyl-bridged RuII/OsII terpyridyl complexes *Angew. Chem., Int. Ed. Engl.* **34** 1100–2
[38] Harriman A and Ziessel R 1996 Making photoactive molecular-scale wires *Chem. Commun.* 1707–16
[39] Ziessel R, Hissler M, El-ghayoury A and Harriman A 1998 Multifunctional transition metal complexes *Coord. Chem. Rev.* **178–80** 1251–98
[40] Borré E, Bellemin-Laponnaz S and Mauro M 2016 Amphiphilic metallopolymers for photoswitchable supramolecular hydrogels *Chem. Eur. J.* **22** 18718–21
[41] Borré E, Stumbé J-F, Bellemin-Laponnaz S and Mauro M 2017 Control of the light-response in supramolecular metallopolymeric gels by tuning the coordination metal *Chem. Commun.* **53** 8344–7
[42] Mauro M 2019 Gel-based soft actuators driven by light *J. Mater. Chem.* B **7** 4234–42
[43] Garah M E, Borré E, Ciesielski A, Dianat A, Gutierrez R, Cuniberti G, Bellemin-Laponnaz S, Mauro M and Samorì P 2017 Light-induced contraction/expansion of 1D photoswitchable metallopolymer monitored at the solid-liquid interface *Small* **13** 1701790
[44] Borré E, Stumbé J-F, Bellemin-Laponnaz S and Mauro M 2016 Light-powered self-healable metallosupramolecular soft actuators *Angew. Chem., Int. Ed. Engl.* **55** 1313–7

[45] Sugimoto K, Tanaka Y, Fujii S, Tada T, Kiguchi M and Akita M 2016 Organometallic molecular wires as versatile modules for energy-level alignment of the metal–molecule–metal junction *Chem. Commun.* **52** 5796–9

[46] Zhang L-Y, Duan P, Wang J-Y, Zhang Q-C and Chen Z-N 2019 Ruthenium(II) as conductive promoter to alleviate conductance attenuation in oligoynyl chains *J. Phys. Chem.* C **123** 5282–8

[47] Saha Roy S, Sil A, Giri D, Roy Chowdhury S, Mishra S and Patra S K 2018 Diruthenium(II)-capped oligothienylethynyl bridged highly soluble organometallic *wires* exhibiting long-range electronic coupling *Dalton Trans.* **47** 14304–17

[48] Tanaka Y, Kato Y, Tada T, Fujii S, Kiguchi M and Akita M 2018 'Doping' of polyyne with an organometallic fragment leads to highly conductive metallapolyyne molecular wire *J. Am. Chem. Soc.* **140** 10080–4

[49] Tanaka Y, Kiguchi M and Akita M 2017 Inorganic and organometallic molecular wires for single-molecule devices *Chem. Eur. J.* **23** 4741–9

[50] Tanaka Y, Koike T and Akita M 2010 Reversible, fine performance tuning of an organometallic molecular wire by addition, ligand replacement and removal of dicobalt fragments *Eur. J. Inorg. Chem.* **2010** 3571–5

[51] Haque A, Al-Balushi R A, Al-Busaidi I J, Khan M S and Raithby P R 2018 Rise of conjugated poly-ynes and poly(metalla-ynes): from design through synthesis to structure–property relationships and applications *Chem. Rev.* **118** 8474–597

[52] Schwarz F, Kastlunger G, Lissel F, Riel H, Venkatesan K, Berke H, Stadler R and Lörtscher E 2014 High-conductive organometallic molecular wires with delocalized electron systems strongly coupled to metal electrodes *Nano Lett.* **14** 5932–40

[53] Meng F, Hervault Y-M, Norel L, Costuas K, Van Dyck C, Geskin V, Cornil J, Hng H H, Rigaut S and Chen X 2012 Photo-modulable molecular transport junctions based on organometallic molecular wires *Chem. Sci.* **3** 3113

[54] Schramm F, Chandrasekar R, Zevaco T A, Rudolph M, Görls H, Poppitz W and Ruben M 2009 (Polypyridyl) ruthenium(II) complexes based on a *back-to-back* bis(pyrazolylpyridine) bridging ligand *Eur. J. Inorg. Chem.* **2009** 53–61

[55] Rajadurai C, Fuhr O, Kruk R, Ghafari M, Hahn H and Ruben M 2007 Above room temperature spin transition in a metallo-supramolecular coordination oligomer/polymer *Chem. Commun.* 2636–8

[56] Attwood M and Turner S S 2017 Back to back 2,6-bis(pyrazol-1-yl)pyridine and 2,2′:6′,2″-terpyridine ligands: Untapped potential for spin crossover research and beyond *Coord. Chem. Rev.* **353** 247–77

[57] Sonogashira K, Tohda Y and Hagihara N 1975 A convenient synthesis of acetylenes: catalytic substitutions of acetylenic hydrogen with bromoalkenes, iodoarenes and bromopyridines *Tetrahedron Lett.* **16** 4467–70

[58] Schütze F, Krumova M and Mecking S 2015 Size control of spherical and anisotropic fluorescent polymer nanoparticles via precise rigid molecules *Macromolecules* **48** 3900–6

[59] Heinz L G, Yushchenko O, Neuburger M, Vauthey E and Wenger O S 2015 Tetramethoxybenzene is a good building block for molecular wires: insights from photoinduced electron transfer *J. Phys. Chem.* A **119** 5676–84

[60] Hofmeier H and Schubert U S 2004 Recent developments in the supramolecular chemistry of terpyridine–metal complexes *Chem. Soc. Rev.* **33** 373–99

[61] James P V, Sudeep P K, Suresh C H and Thomas K G 2006 Photophysical and theoretical investigations of oligo(*p*-phenyleneethynylene)s: effect of alkoxy substitution and alkyne–aryl bond rotations *J. Phys. Chem.* A **110** 4329–37

[62] Klingele J, Kaase D, Schmucker M, Lan Y, Chastanet G and Létard J-F 2013 Thermal spin crossover and LIESST effect observed in complexes $[Fe(L^{Ch})_2(NCX)_2]$ [L^{Ch} = 2,5-Di(2-Pyridyl)-1,3,4-chalcadiazole; Ch = O, S, Se; X = S, Se, BH_3] *Inorg. Chem.* **52** 6000–10

[63] Nacci C, Ample F, Bleger D, Hecht S, Joachim C and Grill L 2015 Conductance of a single flexible molecular wire composed of alternating donor and acceptor units *Nat. Commun.* **6** 7397

[64] Weiss E A, Ahrens M J, Sinks L E, Gusev A V, Ratner M A and Wasielewski M R 2004 Making a molecular wire: charge and spin transport through *p ara* -phenylene oligomers *J. Am. Chem. Soc.* **126** 5577–84

[65] London A E *et al* 2019 A high-spin ground-state donor-acceptor conjugated polymer *Sci. Adv.* **5** eaav2336

[66] Liu Z, Ren S and Guo X 2019 Switching effects in molecular electronic devices *Molecular-Scale Electronics* ed X Guo (Cham: Springer) pp 173–205

[67] Vezzoli A, Grace I M, Brooke C, Nichols R J, Lambert C J and Higgins S J 2017 Soft versus hard junction formation for α-terthiophene molecular wires and their charge transfer complexes *J. Chem. Phys.* **146** 092307

[68] Lissau H, Frisenda R, Olsen S T, Jevric M, Parker C R, Kadziola A, Hansen T, van der Zant H S J, Brøndsted Nielsen M and Mikkelsen K V 2015 Tracking molecular resonance forms of donor–acceptor push–pull molecules by single-molecule conductance experiments *Nat. Commun.* **6** 10233

[69] Sakamoto R, Katagiri S, Maeda H and Nishihara H 2013 Bis(terpyridine) metal complex wires: excellent long-range electron transfer ability and controllable intrawire redox conduction on silicon electrode *Coord. Chem. Rev.* **257** 1493–506

[70] Bajpayee A, Maeda H, Katagiri S, Sakamoto R and Nishihara H 2015 Bis(terpyridine)iron(II) complex wires with a bithiophene linker for superior long-range electron transport *Chem. Lett.* **44** 1211–3

[71] Sakamoto R, Katagiri S, Maeda H, Nishimori Y, Miyashita S and Nishihara H 2015 Electron transport dynamics in redox-molecule-terminated branched oligomer wires on Au(1 1 1) *J. Am. Chem. Soc.* **137** 734–41

[72] Sakamoto R, Ohirabaru Y, Matsuoka R, Maeda H, Katagiri S and Nishihara H 2013 Orthogonal bis(terpyridine)–Fe(ii) metal complex oligomer wires on a tripodal scaffold: rapid electron transport *Chem. Commun.* **49** 7108

[73] Katagiri S, Sakamoto R, Maeda H, Nishimori Y, Kurita T and Nishihara H 2013 Terminal redox-site effect on the long-range electron conduction of $Fe(tpy)_2$ oligomer wires on a gold electrode *Chem. Eur. J.* **19** 5088–96

[74] Sakamoto R, Wu K-H, Matsuoka R, Maeda H and Nishihara H 2015 π-conjugated bis(terpyridine)metal complex molecular wires *Chem. Soc. Rev.* **44** 7698–714

[75] Rigaut S 2013 Metal complexes in molecular junctions *Dalton Trans.* **42** 15859

[76] Nitzan A 2003 Electron transport in molecular wire junctions *Science* **300** 1384–9

[77] Mujica V, Nitzan A, Datta S, Ratner M A and Kubiak C P 2003 Molecular wire junctions: tuning the conductance *J. Phys. Chem.* B **107** 91–5

[78] Emberly E G and Kirczenow G 2002 Molecular spintronics: spin-dependent electron transport in molecular wires *Chem. Phys.* **281** 311–24

[79] Kasibhatla B S T, Labonté A P, Zahid F, Reifenberger R G, Datta S and Kubiak C P 2003 Reversibly altering electronic conduction through a single molecule by a chemical binding event *J. Phys. Chem.* B **107** 12378–82

[80] Zhang Y, Ye Y, Li Y, Yin X, Liu H and Zhao J 2007 Ab initio investigations of quaterthiophene molecular wire under

the interaction of external electric field *J. Mol. Struct. Theochem.* **802** 53–8
[81] Hu W, Nakashima H, Furukawa K, Kashimura Y, Ajito K, Han C and Torimitsu K 2004 Carrier injection from gold electrodes into thioacetyl-end-functionalized poly(*para* -phenyleneethynylene)s *Phys. Rev.* B **69** 165207
[82] Girlandal M, Cacelli I, Ferretti A and Macucci M 2004 Conductance modulation in molecular devices via field-induced conformational change *4th IEEE Conf. on Nanotechnology, 2004* (Munich: IEEE) pp 131–3
[83] Bullard G, Tassinari F, Ko C-H, Mondal A K, Wang R, Mishra S, Naaman R and Therien M J 2019 Low-resistance molecular wires propagate spin-polarized currents *J. Am. Chem. Soc.* **141** 14707–11
[84] Sun Y-Y, Peng Z-L, Hou R, Liang J-H, Zheng J-F, Zhou X-Y, Zhou X-S, Jin S, Niu Z-J and Mao B-W 2014 Enhancing electron transport in molecular wires by insertion of a ferrocene center *Phys. Chem. Chem. Phys.* **16** 2260
[85] Abhervé A, Mañas-Valero S, Clemente-León M and Coronado E 2015 Graphene related magnetic materials: micromechanical exfoliation of 2D layered magnets based on bimetallic anilate complexes with inserted $[Fe^{III}(acac_2\text{-trien})]^+$ and $[Fe^{III}(sal_2\text{-trien})]^+$ molecules *Chem. Sci.* **6** 4665–73
[86] Suárez-García S, Adarsh N N, Molnár G, Bousseksou A, Garcia Y, Dîrtu M M, Saiz-Poseu J, Robles R, Ordejón P and Ruiz-Molina D 2018 Spin-crossover in an exfoliated 2D coordination polymer and its implementation in thermochromic films *ACS Appl. Nano Mater.* **1** 2662–8
[87] Bhat G A, Haldar S, Verma S, Chakraborty D, Vaidhyanathan R and Murugavel R 2019 Facile exfoliation of single-crystalline copper alkylphosphates to single-layer nanosheets and enhanced supercapacitance *Angew. Chem., Int. Ed. Engl.* **18** 16844–9
[88] Lefter C, Davesne V, Salmon L, Molnár G, Demont P, Rotaru A and Bousseksou A 2016 Charge transport and electrical properties of spin crossover materials: towards nanoelectronic and spintronic devices *Magnetochemistry* **2** 18
[89] Meded V, Bagrets A, Fink K, Chandrasekar R, Ruben M, Evers F, Bernand-Mantel A, Seldenthuis J S, Beukman A and van der Zant H S J 2011 Electrical control over the Fe(II) spin crossover in a single molecule: Theory and experiment *Phys. Rev.* B **83** 245415
[90] Ruben M, Rojo J, Romero-Salguero F J, Uppadine L H and Lehn J-M 2004 Grid-type metal ion architectures: functional metallosupramolecular arrays *Angew. Chem., Int. Ed. Engl.* **43** 3644–62
[91] Ruben M, Breuning E, Lehn J-M, Ksenofontov V, Renz F, Gütlich P and Vaughan G B M 2003 Supramolecular spintronic devices: spin transitions and magnetostructural correlations in$[Fe_4IIL_4]8 + [2 \times 2]$-grid-type complexes *Chem. Eur. J.* **9** 4422–9
[92] Gopakumar T G, Matino F, Naggert H, Bannwarth A, Tuczek F and Berndt R 2012 Electron-induced spin crossover of single molecules in a bilayer on gold *Angew. Chem., Int. Ed. Engl.* **51** 6262–6
[93] Miyamachi T *et al* 2012 Robust spin crossover and memristance across a single molecule *Nat. Commun.* **3** 938
[94] Schleicher F *et al* 2018 Linking electronic transport through a spin crossover thin film to the molecular spin state using x-ray absorption spectroscopy operando techniques *ACS Appl. Mater. Interfaces* **10** 31580–5